Perspectives for the understanding of complex deposits on surfaces

Christophe Henry [1]

[1]Instytut Maszyn Przepływowych, Polska Akademia Nauk
(Institute of Fluid-Flow Machinery, Polish Academy of Sciences)
ul. Fiszera 14, 80-231 Gdańsk, Poland

Instytut Podstawowych Problemów Techniki, Polskiej Akademii Nauk
Institute of Fundamental Technological Research, Polish Academy of Sciences
April 8th, 2015

General field of research: particulate fouling

- Study of **particulate fouling**, i.e. the accumulation of solid inorganic particles on a surface
  focus on spherical **colloidal particles**

- Example of systems affected by particulate fouling:
  - Fouling in heat exchangers (reduction of heat transfer efficiency)
  - Fouling in the automotive industry (by soot particles in combustion engines)

- Other possible sources of fouling:
  - Fouling in the membrane filtration (organic macromolecules in water treatment facilities)
  - Fouling in the medical field (blood vessel clogging, deposition in human lungs, contaminant resuspension in hospitals)

Table of contents

Plan

Guidelines to study particulate fouling

- Fouling can be described with 4 underlying phenomena:

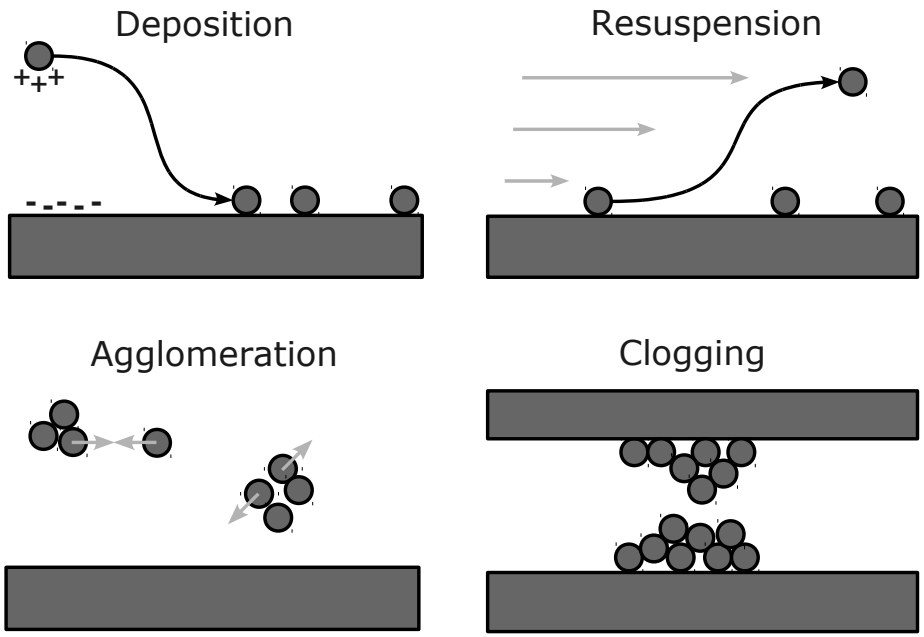

- Three key interactions at play:
  particle-fluid, particle-particle and particle-surface interactions
- Interplay between two fundamental mechanisms:
  1. **Transport step**: hydrodynamic transport of particles to the surface
  2. **Attachment step**: adhesion due to the particle-surface interaction

Plan

Experimental evidence of particle deposition

- Analysis of experimental data available
  (see *Henry et al, Adv. Colloid Interface Sci., 2012, Vol. 185-186, pp. 34-76*)
  - Evolution of the deposition rate with fluid (velocity, pH, ionic strength), particle (concentration, size, potential) and wall (potential, roughness) properties

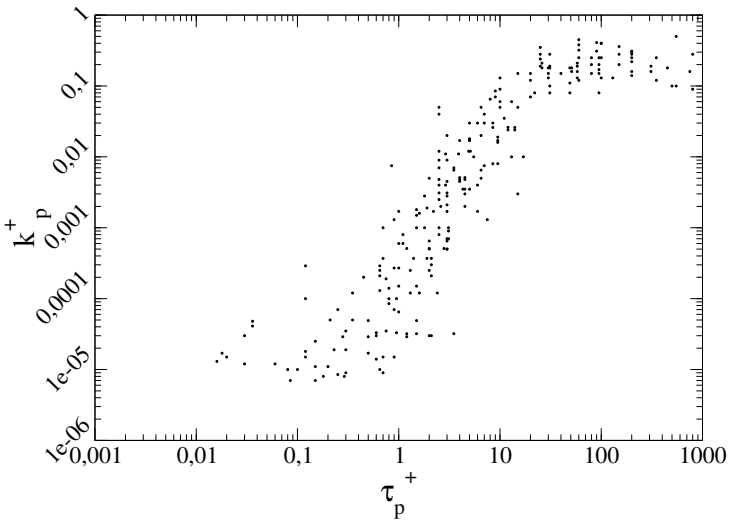

(a) Compilation of various experimental data on the deposition rate (from Papavergos & Hedley, Chem Eng Res Des, 1984)

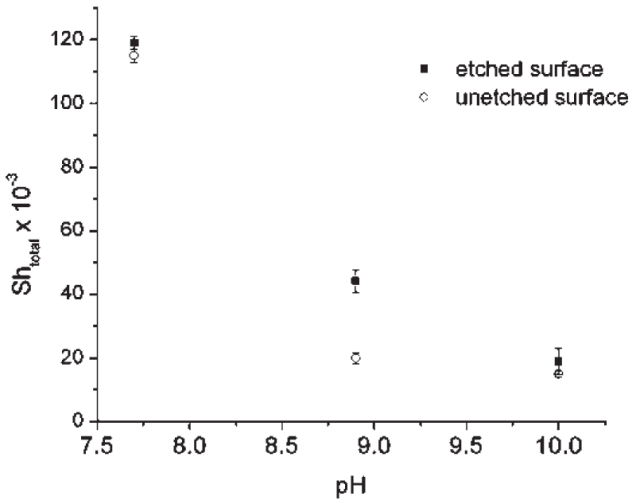

(b) Sherwood number for latex particles depositing on calcite surfaces expressed as a function of pH (from Darbha et al., Langmuir, 2010)

Experimental evidence of particle deposition (2)

- Analysis of experimental data available
  (see *Henry et al, Adv. Colloid Interface Sci., 2012, Vol. 185-186, pp. 34-76*)
  - Evolution of the deposition rate with fluid (velocity, pH, ionic strength), particle (concentration, size, potential) and wall (potential, roughness) properties
  - Three typical features for the deposit morphology

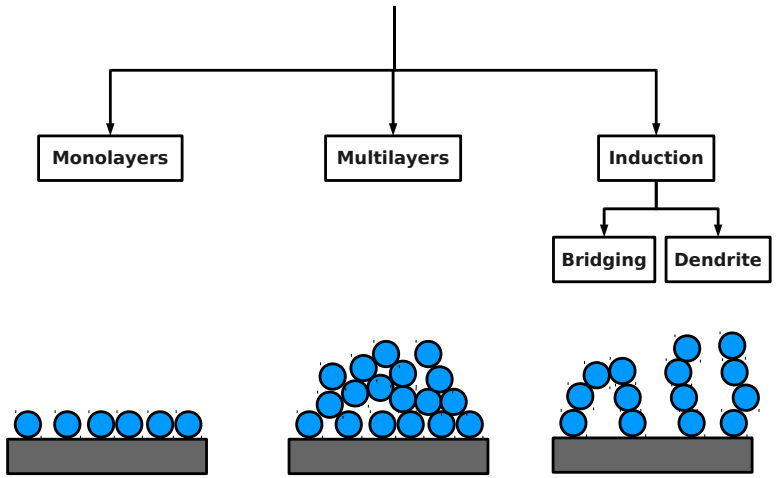

$\Rightarrow$ Intricate coupling between **particle-fluid**, **particle-surface** and **particle-particle** interactions

Modelling approaches for particle deposition

Various levels of description for the particle phase:

- Adsorption model (no fluid):
  RSA or Ballistic models (to generate random packing of particles)
- Models for particle transport with fluid
  - Lagrangian approaches:
    Explicit tracking of particles with a complexity (and computational cost) that depends on the level of description of particle motion
    - MD Methods
    - Discrete Element Methods
    - Langevin Dynamics
    - Brownian Dynamics
    - Dissipative Particle Dynamics
    - One-particle pdf approach
  - Lattice-Boltzmann Methods
  - Eulerian approaches:
    Fast evaluations of macroscopic properties (particle concentration),
    but requires proper formula for the deposition rate (boundary condition)

A one-point pdf formulation for particle deposition (1)

Description by a two-step process:

- **A transport step**:
  - Modelled following the work of *Minier and Peirano, Phys. Rep., 2001, Vol. 352, pp. 1-214*:
    $\rightarrow$ Eulerian calculation of the fluid phase (RANS calculation)
    $\rightarrow$ Lagrangian tracking of particles (stochastic method)

    Evolution of each particle state-vector $\mathbf{Z} = (\mathbf{x_p}, \mathbf{U_p}, \mathbf{U_s})$
    $\mathbf{x_p}$: particle position, $\mathbf{U_p}$: particle velocity, $\mathbf{U_s}$: velocity of the fluid seen by particles along their trajectory
    Use of a Langevin equation

$$dx_{p,i} = U_{p,i}dt$$
$$dU_{p,i} = \frac{U_{s,i} - U_{p,i}}{\tau_p}dt + K_{Br}dW_i' + (gdt)$$
$$dU_{s,i} = A_i(t, U_{s,i})dt + B_i(t, U_{s,i})dW_i$$

  - Refinement accounting for interactions of particles with the near-wall coherent structures *Guingo and Minier, Phys. Fluids, 2008, Vol. 20, 053303*
  - **Validated on several configurations**

A one-point pdf formulation for particle deposition (2)

Description by a two-step process:

- **A transport step**:
  - Modelled following the work of *Minier and Peirano, Phys. Rep., 2001, Vol. 352, pp. 1-214*:
    $\rightarrow$ Eulerian calculation of the fluid phase (RANS calculation)
    $\rightarrow$ Lagrangian tracking of particles (stochastic method)
  - Refinement accounting for interactions of particles with the near-wall coherent structures *Guingo and Minier, Phys. Fluids, 2008, Vol. 20, 053303*
  - **Validated on several configurations**

- **An attachment step**:
  - Particle-surface interactions modelled using the DLVO theory (Derjaguin and Landau, Verwey and Overbeek) which accounts for:
    - van der Waals forces
    - electrostatic forces
  - Refinements accounting for the presence of surface roughness:

Smooth plate with hemispherical asperities
Additivity of interaction energies

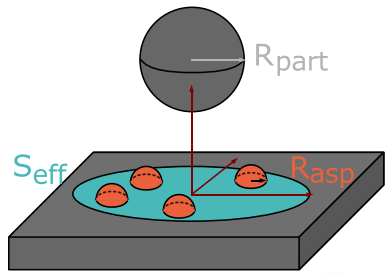

A one-point pdf formulation for particle deposition (3)

Description by a two-step process:

- **A transport step**:
  - Modelled following the work of *Minier and Peirano, Phys. Rep., 2001, Vol. 352, pp. 1-214*:
    $\rightarrow$ Eulerian calculation of the fluid phase (RANS calculation)
    $\rightarrow$ Lagrangian tracking of particles (stochastic method)
  - Refinement accounting for interactions of particles with the near-wall coherent structures *Guingo and Minier, Phys. Fluids, 2008, Vol. 20, 053303*
  - **Validated on several configurations**

- **An attachment step**:
  - Particle-surface interactions modelled using the DLVO theory (Derjaguin and Landau, Verwey and Overbeek) which accounts for:
    - van der Waals forces
    - electrostatic forces
  - Refinements accounting for the presence of surface roughness

- **Coupling using an energetic approach** due to different scales involved:
  $\rightarrow$ Comparison of the kinetic energy E_{Kin} and the energy barrier E_{Barr} (maximum repulsive interaction obtained with a DLVO calculation)

Single particle deposition (1)

- Numerical results obtained for single particle deposition
  - Introduction of surface roughness in particle-surface interactions
  - Analysis of the effect of surface roughness on particle-surface interactions
  - Validation of the new model by comparison with experimental data

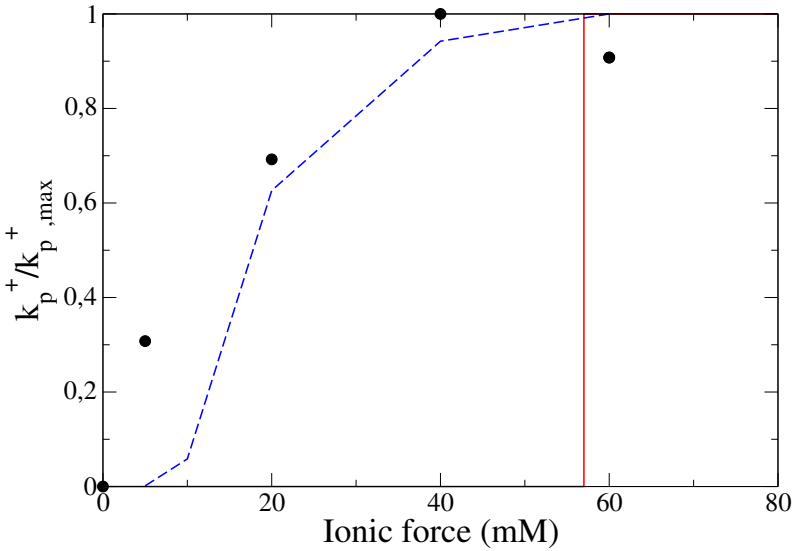

Normalized deposition rate of 0.8 μm polystyrene particles on PMMA surfaces (experimental data from *Sjollema and Busscher, Colloids & Surfaces, 1990*)

(•) experimental measurements,
(—) numerical results on smooth surface,
(- -) numerical results for rough surfaces (5 up to 50nm covering 8% of the surface)

$\Rightarrow$ **Non-zero deposition rates in repulsive conditions are reproduced**

Single particle deposition (2)

- Numerical results obtained for single particle deposition
  - Introduction of surface roughness in particle-surface interactions
  - Analysis of the effect of surface roughness on particle-surface interactions
  - Validation of the new model by comparison with experimental data

Deposition of hematite particles on polypropylene (*Čerović et al, J. Colloid Interface Sci., 2009*)

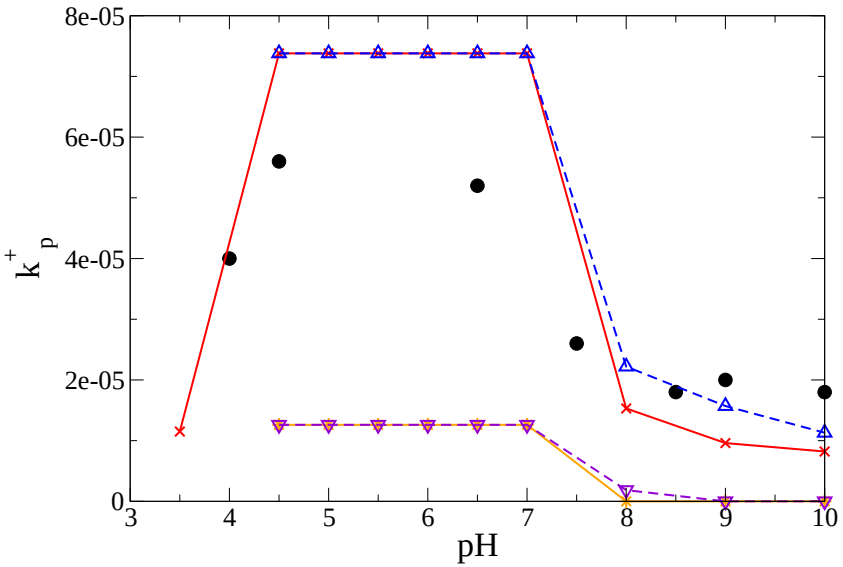

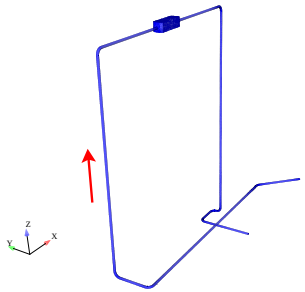

(•) experimental measurements,

numerical results on the whole loop
(×) with smooth surfaces,
(△) with rough surfaces.

numerical results on a simple pipe
(⋆) with smooth surfaces,
(▽) with rough surfaces.

⇒ **The overall deposition rate is increased by singularities (bends, box)**

Multilayer deposition (1)

- Extension of the model for multilayer deposition
  - Development of a new modelling approach to clogging
    - Assumptions made for the first modelling steps:

      → Dilute suspension
      → No reentrainment
      → No influence of deposits on the fluid

    - Use of a two-step process with an energy-balance approach for the coupling of both steps (similar to deposition):

      → **Unchanged transport step** (no fluid motion around deposits): modelled using the same stochastic Lagrangian approach already used for hydrodynamic transport of particles
      → **Modified attachment step** (to account for particle-particle interactions): modelled using the DLVO theory and a statistical description of the fouled surface (surface covered by deposited particles, size of deposited particles).

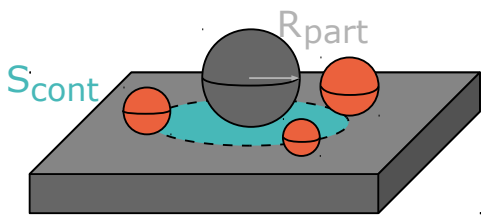

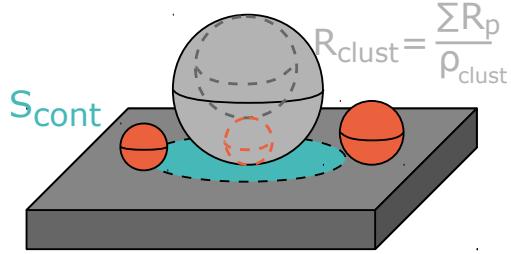

Multilayer deposition (2)

- Extension of the model for multilayer deposition
  - Development of a new modelling approach to clogging
  - Qualitative validation of the new modelling approach

    250 *nm* alumina particles on silicon susbtrates (data from *Perry et al, Microfluid Nanofluid, 2008*): Only one layer at $pH = 3$, Multilayer deposit at $pH = 9$ and 9.5, No fouling at $pH \geq 10$

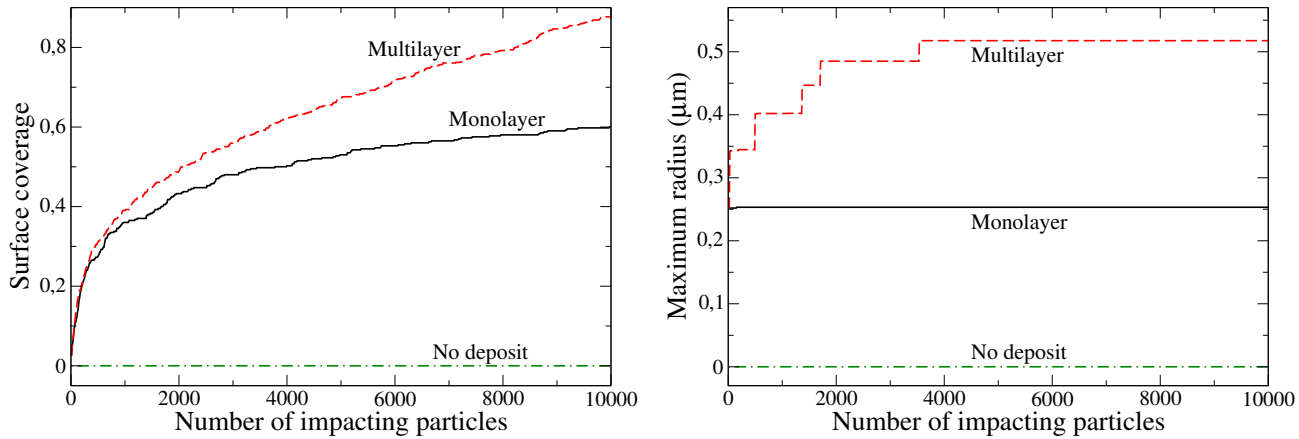

(c) Surface covered by particles (d) Maximum particle/cluster size

Figure : Numerical results for the clogging behaviour of silicon substrates by alumina particles: – pH 3, - - pH 9, ·– pH 10

Multilayer deposition (3)

- Extension of the model for multilayer deposition
  - Development of a new modelling approach to clogging
  - Possibility to simulate channel blockage

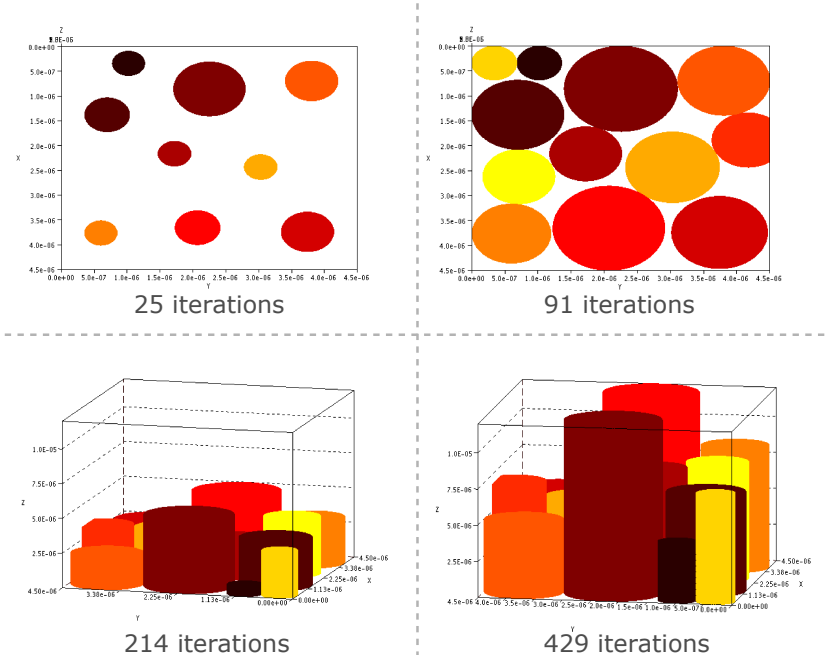

Figure : Clogging of a microchannel through sequential deposition of small particles (a,b,c) until the flow passage becomes blocked by a larger particle (d)

⇒ **Tractable simulations in 3-D cases until complete flow blockage**

Plan

Experimental evidence of resuspension mechanisms

- Two different mechanisms

Rolling motion (mainly small particles)

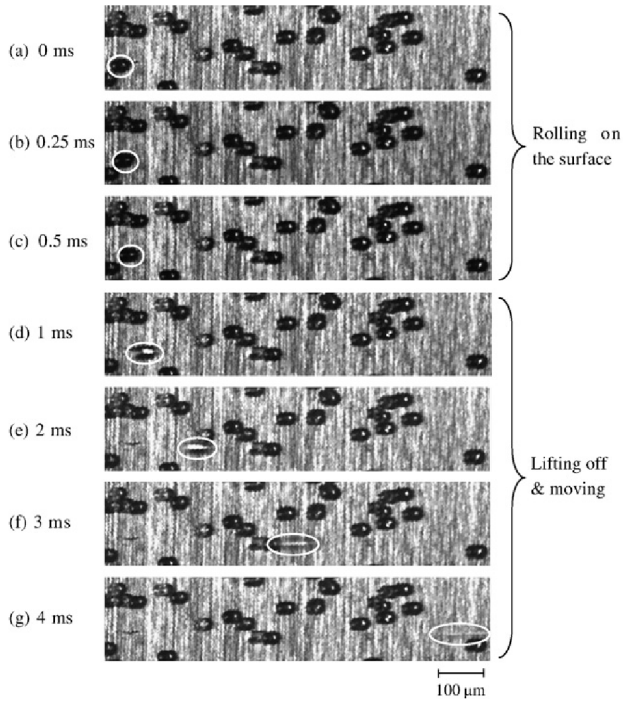

Figure : Snapshots of an entrained glass particle ($d_p = 30\ \mu m$, $d_p^+ = 7$) from a rough substrate as recorded by Jiang et al. (from Jiang et al., Pow Tec, 2008)

'Burst-type' resuspension (large particles)

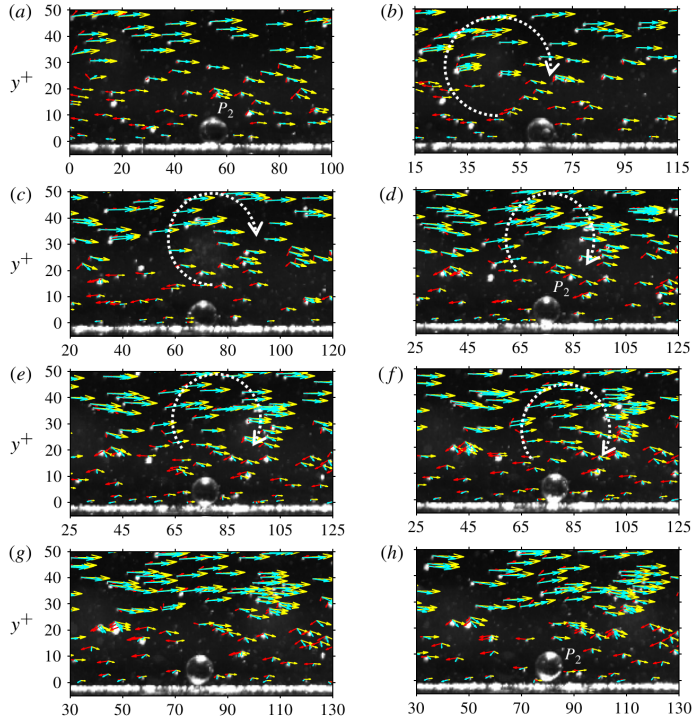

Figure : Sequence of PIV images superposed with PTV vectors showing the resuspension of a polystyrene particle ($d_p = 538\ \mu m$, $d_p^+ = 10$) (from van Hout, J Fluid Mech, 2013)

Modelling approaches for particle resuspension

Various models depending on the level of description of particle dynamics

- Empirical formulas:
  Providing macroscopic information (useful in Eulerian approaches)
  but highly dependent on the conditions studied
- Force-balance approach
  Reentrainment due to the rupture of equilibrium (lift, rolling or sliding motion)
  Adapted for both Lagrangian and Eulerian (extraction of macroscopic laws) calculations
- Kinetic PDF approaches (RRH, Rock'n'Roll theories)
  Reentrainment due to oscillations around the contact point due to turbulent fluid fluctuations
- Dynamic PDF approaches
  Reentrainment accounting for the whole dynamics of rolling particles
- DEM methods
  Possibility of performing very fine calculations with rolling, sliding and lifting motions

A one-point PDF approach for colloidal resuspension

- **Model**
  - Introduction of surface roughness for adhering particle-surface contact forces
  - Mechanism retained for particle resuspension: **rolling motion**

    Analysis of the effect of surface roughness on the reentrainment process
    → Reduction of adhesion energies with nanoscale roughness
    → Rocking of particles on microscale roughness

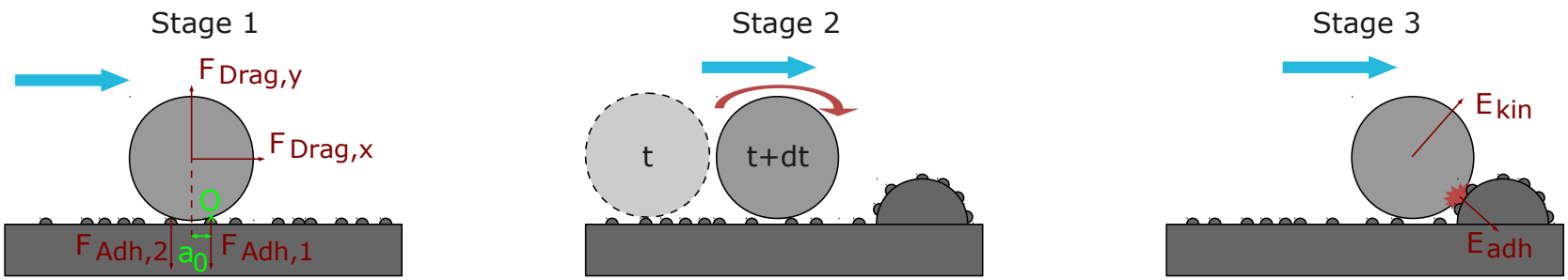

Equation of particle motions:
Streamwise velocity approximated using the angular velocity: $U_{p,//} \simeq R_{part}\,\omega$
Angular velocity given by the balance between moments exerted on particles:

$$I\frac{d\omega}{dt} \simeq M_O(F_{drag,//}) - M_O(F_{adh})$$

with $I = 7m_{part}R_{part}^2/5$ the moment of inertia, $M_O(F_{drag,//}) = 1.4 \times R_{part} \times F_{drag,//}$ and $M_O(F_{adh}) = F_{adh} \times a_0$ the hydrodynamic and adhesion moments

Results obtained on particle reentrainment (1)

- Numerical results obtained with the one-point PDF approach
  - Introduction of surface roughness for adhering particle-surface contact forces (see *Henry et al, Langmuir, 2012, Vol. 28, pp. 438-452*)

    Statistical description of surface roughness using R_{asp} and S_{cov}
    $\rightarrow$ Statistical information on the adhesion force (or energy)

    Validated on several test cases:
    For instance, adhesion between 10 μm polystyrene particles and aluminum polished substrate: • experimental data (from *Zhou et al., Powder Technol, 2003, Vol. 135-136, 82-91*), – predictions with $R_{asp} = 250\ nm$ ($S_{cov} = 0.5$ %)

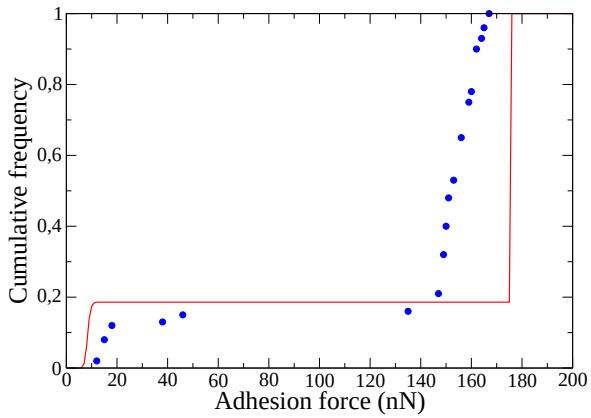

    $\Rightarrow$ Possibility to retrieve complex distributions of the adhesion force

Main results obtained for particle resuspension

- Numerical results obtained with the one-point PDF approach
  - Introduction of surface roughness for adhering particle-surface contact forces
  - Validation of the new model by comparison with experimental data

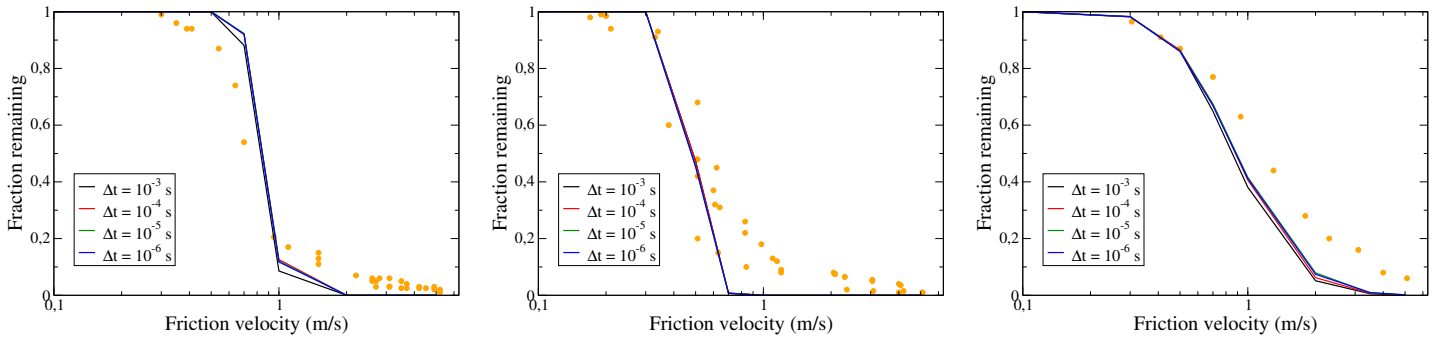

(a) 10 μm alumina (b) 20 μm alumina (c) 13 μm graphite

Figure : Fraction of alumina or graphite particles remaining on stainless steel substrates after a 1 s exposure to an airflow with varying friction velocity:
• experimental data (from *Reeks et al, Aerosol Sci., 2001, Vol. 32, pp. 1-31*)
numerical results ($R_{asp}^{large} = 2\ \mu m, S_{cov}^{large} = 3.1\ \%$ and $R_{asp}^{small} = 5\ nm, S_{cov}^{small} = 3\ \%$)

$\Rightarrow$ **Relatively correct predictions of particle resuspension from rough substrates**

Plan

State-of-the-art in the formation of complex deposits

- Relatively extensive experimental data on deposition and resuspension from monolayers
- Satisfactory predictions provided that modelling approaches properly account for the coupling between hydrodynamic transport, physico-chemistry of interfaces as well as with surface roughness

$\Rightarrow$ **Importance of having accurate and consitent descriptions of particle-fluid, particle-surface and particle-particle interactions**

Table of contents

Plan

Deposit morphology

- Experimental data:
  - Recent experimental data in microfluidics on the growth of complex deposits with colloidal particles
  - Existing works on the formation of deposits for large particles (dust, sand, etc.)
    $\Rightarrow$ Characterisation of the morphology in terms of fractal dimension d_F, coordination number N_C, porosity ρ, etc.
  - But **lack of information** on the evolution of the deposit morphology with fluid, particle and surface properties (especially for colloidal particles)
    $\Rightarrow$ Need of experimental study similar to those already done for particle agglomeration and fragmentation
  - Need of experimental studies the mechanisms at play in the formation of a given deposit morphology
    $\rightarrow$ how particles stick to a deposited cluster? Do they stick immediately or roll for a certain time? To what extent these mechanisms impact the morphology?

Deposit morphology

- Modelling approaches:
  - Recent breakthrough in the effect of fluid velocity and particle-particle interactions on the deposit morphology using very fine Lagrangian methods (often DEM)
  - Limitation of such DEM simulations:
    particle either stick or roll until reaching a stable position
    No effect of surface roughness on rolling motion (possibly leading to different PDF of the contact angle between particles)

    $\rightarrow$ **need to include the effect of surface roughness** in such methods, or to use multi-scale approaches (PDF of the contact angle given by a finer calculation)

Deposit cohesion

Need of experimental (and later numerical) studies on several topics:

- Cohesion forces and deformation:

  Need to quantify the role played by surface deformation in cohesion forces with respect to particle size and nature (properties).

  Importance of plastic deformation (which requires development of new contact theories)?

- Restructuring:

  Need to evaluate the role played by deposit restructuring for colloidal particles (largely studied in the case of large inertial particles such as sand)
  $\rightarrow$ Is restructuring realistic for colloidal particle with low energy at impact?
  Possibility to study these effects in particle agglomeration/fragmentation

Deposit consolidation (1)

- Experimental evidence of deposit consolidation:
  - Consolidation in heat exchangers (superheaters, nuclear power plants, ...)
  - Ash deposit in gasifiers:

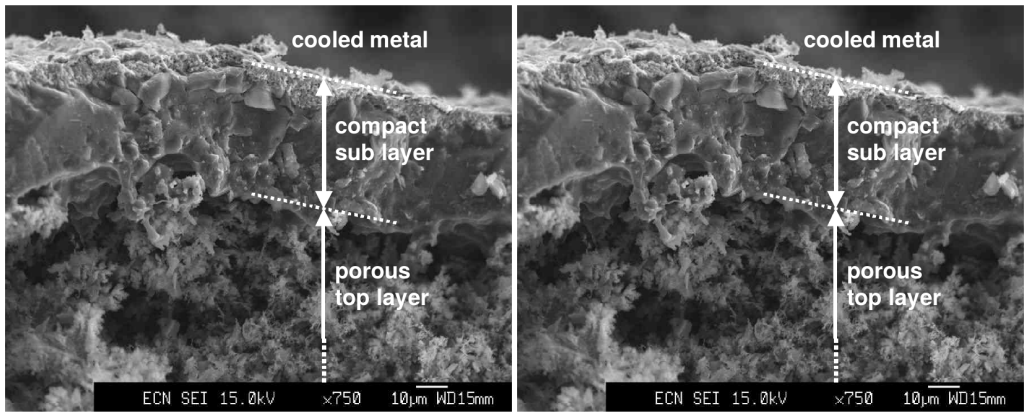

Figure : Deposit formed on a cool surface (from Drift&Pels, ECN-04-077) showing a compact layer (ash particles and condensated tar) and a porous layer (char particles)

- Various possible mechanisms for consolidation:
  - Ostwald ripening
  - Dissolution/precipitation of oxides in solution
  - Sintering
  - Boiling-induced precipitation

Deposit consolidation (2)

- Model for particle consolidation
  - Complexity and variety of mechanisms involved
  - Lack of fine (microscopic) numerical/experimental studies of consolidation phenomena
  - Existing models are restricted to macroscopic effects related to consolidation (mostly thermal conductivity)
- Constraints related to the Lagrangian module in *Code_Saturne*
  - No detailed information on the cluster structure

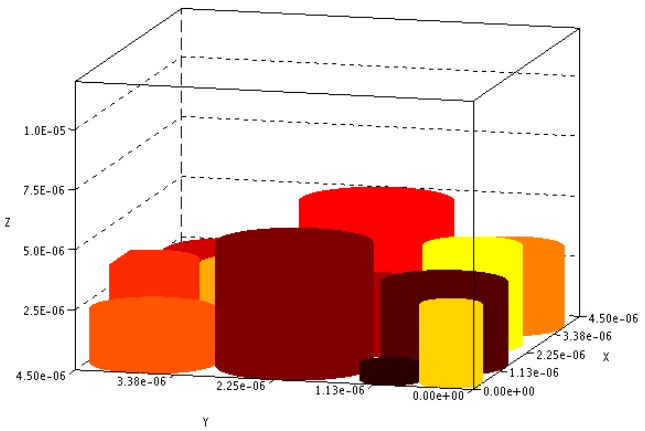

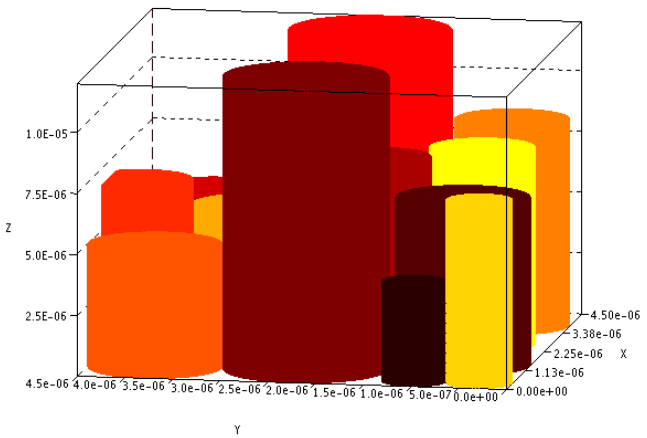

Deposit consolidation (3)

- Model for particle consolidation
  - Evolution of the force between particles as a function of the cluster time since deposition and cluster height

$$F_{adh}^{p-p} = F_{adh,DLVO}^{p-p} \times (1 - f(h,t)) + F_{consol}^{p-p} \times f(h,t)$$

$$f(h,t) = 0.5 \times \left(1 - tanh\left[\frac{h - h_{consol}}{k_{consol} \times h_{consol}}\right]\right)$$

with h_{consol} the height of consolidated deposits at time t
and $k_{consol} = 0.1$ ($k_{consol} \to 0$ for structures with only two layers)

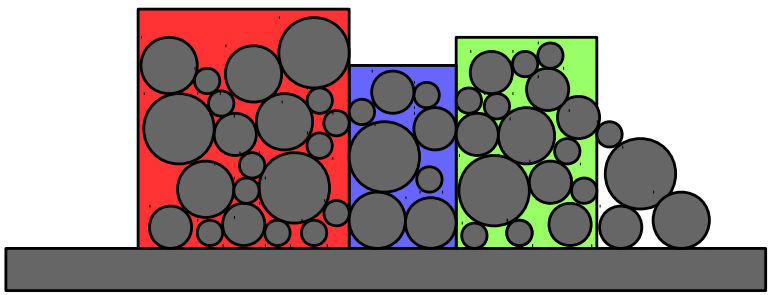

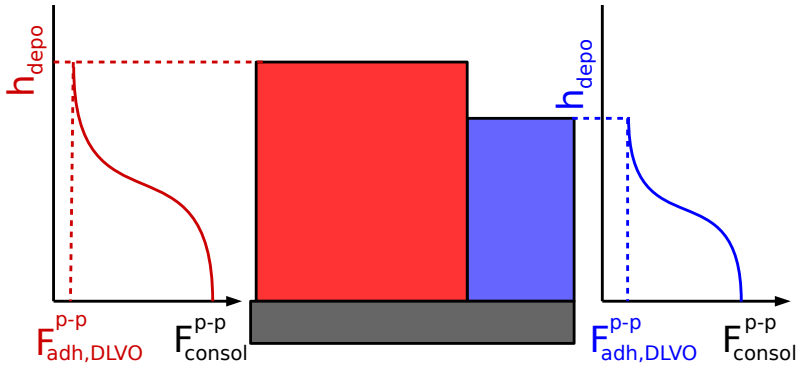

⇒ Need for detailed experimental/numerical studies on consolidation to provide the evolution of inter-particle forces in clusters

Plan

Two-way coupling

- Experiments:
  - Need of fine measurements of the effect of complex colloidal deposits on fluid motions and near-wall turbulence (using PIV/PTV methods)

Two-way coupling

- Modelling approaches
  - DNS with finite-sized particles:
    ⇒ Exact calculation of particle motions, but high computational costs
  - Moving boundary approach:
    ⇒ Particle motion around smoothed surfaces, but complex evolution with resuspension
  - Porous media (for Eulerian calculations of the fluid):
    ⇒ Modifications of the fluid motions at the mesh scale using Darcy law:

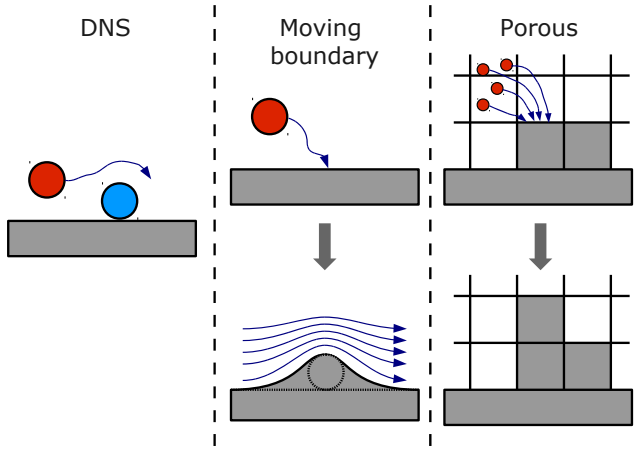

⇒ **Need for a consistency between the calculation of particle and fluid phases**

Plan

Multilayer resuspension

- Coupling between various mechanisms:
  - Hydrodynamic multilayer resuspension
  - Resuspension after impaction
  - Fragmentation after impaction

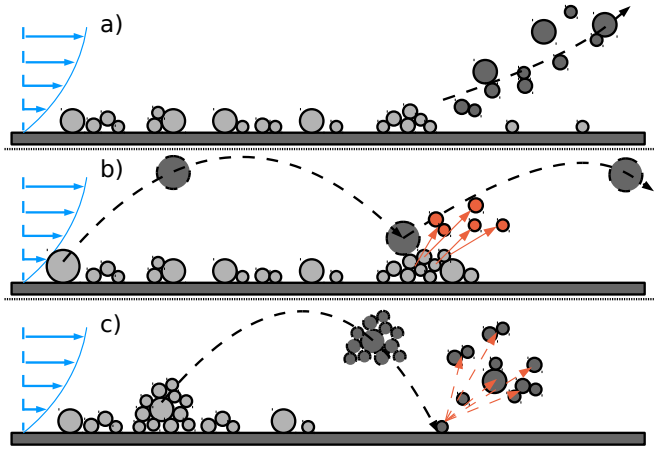

Figure : Illustration of the three dust emission mechanisms proposed by Kok et al., Rep Prog Phys, 2012

Multilayer resuspension

- Hydrodynamic multilayer resuspension
  - Experimental data:
    Smaller particles are harder to remove
    Breakage of clusters around weak cohesion zones
    ⇒ complex dependence on deposit morphology and intricate screening/hiding effects

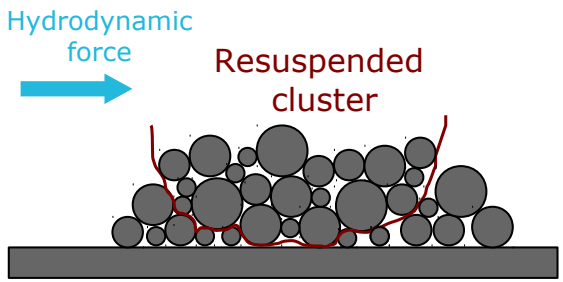

  - Modelling approaches:
    Empirical models
    Extended kinetic PDF approaches (accounting for changes of hydrodynamic/adhesion forces with the layer number)
    Fine DEM methods (with rotational and translational motion)

Figure : Snapshots of particle reentrainment from an initially nearly spherical cluster exposed to shear flow (from Iimura et al., Chem Eng Sci, 2009)

Multilayer resuspension

- Resuspension after impaction (or splashing)
  - Experimental data:
    Mostly for **large cohesionless particles** (sediments, sand, dusts)
    High speed video recording

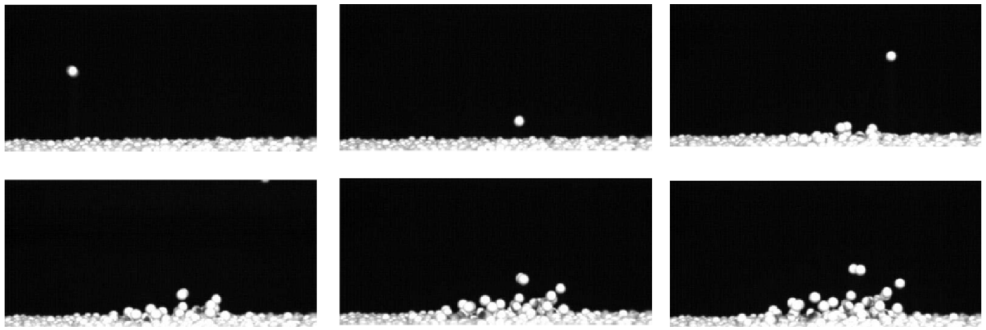

Figure : High-speed images of the splashing of millimetres particles: the time between two images is 4 *ms* (from Beladjine et al., Phys Rev E, 2007)

  - Modelling approaches
    DEM with force/energy propagation

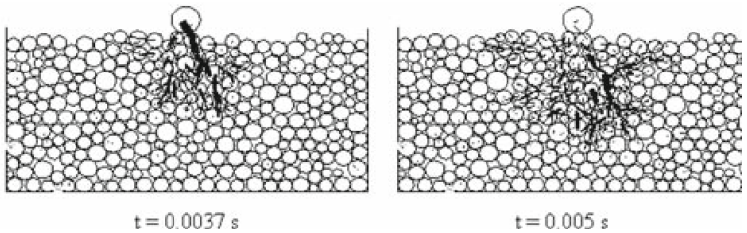

Figure : Snapshots of compression wave propagation obtained with a 2D DEM model (from Bourrier, Gran Mat, 2008)

Multilayer resuspension

- Fragmentation after impaction
  - Recent experimental data (2007):
    Mostly on **colloidal particles** (significant adhesion forces)
    Characterisation of agglomerate after impact using TEM showing the effect of impact velocity, agglomerate structure (compact agglomerates are harder to break), deposit nature
  - Modelling approaches:
    MD-like methods

$\Rightarrow$ Dependence of splashing and impact fragmentation on several properties: impacting particle (velocity, angle), deposit (structural ordering, visco-elastic properties)

Multilayer resuspension

- Limitations and perspectives
  - Need of fine PIV/PTV measurements to highlight the mechanisms (rolling, sliding, lifting?) of multilayer resuspension

    $\Rightarrow$ development of refined models (DEM, dynamic PDF)

  - Need of experimental data for splashing with colloidal particles (if significant) and coupling between splashing and impact fragmentation

  - Experimental quantification of the **relative importance** of hydrodynamics, splashing and impact fragmentation in multilayer resuspension both for colloidal and large inertial particles

    $\Rightarrow$ Refinement of modelling approaches (DEM, dynamic PDF) to account for the whole range of possible mechanisms

Acknowlegments

- Thanks to:
  - Jean-Pierre Minier, EDF R&D - MFEE, Chatou, France
  - Jacek Pozorski, IMP PAN, Gdańsk, Poland
  - Grégory Lefèvre, LECIME - Chimie ParisTech, Paris, France

Further readings

- Henry C. et al., Langmuir, 2011, Vol. 27, pp. 4603-4612
- Henry C. et al., Langmuir, 2012, Vol. 28, pp. 438-452
- Henry C. et al., Advances in Colloid and Interface Science, 2012, Vol. 185-186, pp. 34-76
- Henry C. and Minier J.-P., 2014, Progress in Energy and Combustion Science, Vol. 45, pp. 1-53
- Henry C. and Minier J.-P., 2014, Journal of Aerosol Science, Vol. 77, pp. 168-192

Thank you for your attention

Any question?

Appendix

- General remarks and definitions
- Particle-fluid interactions
  - Modelling of the fluid phase
  - Modelling approaches for particle motions
  - One-particle PDF approach
- Particle-surface interactions
  - DLVO theory
  - Accounting for surface roughness
  - Other parameters influencing adhesion
  - Contact forces

Size separation of particles

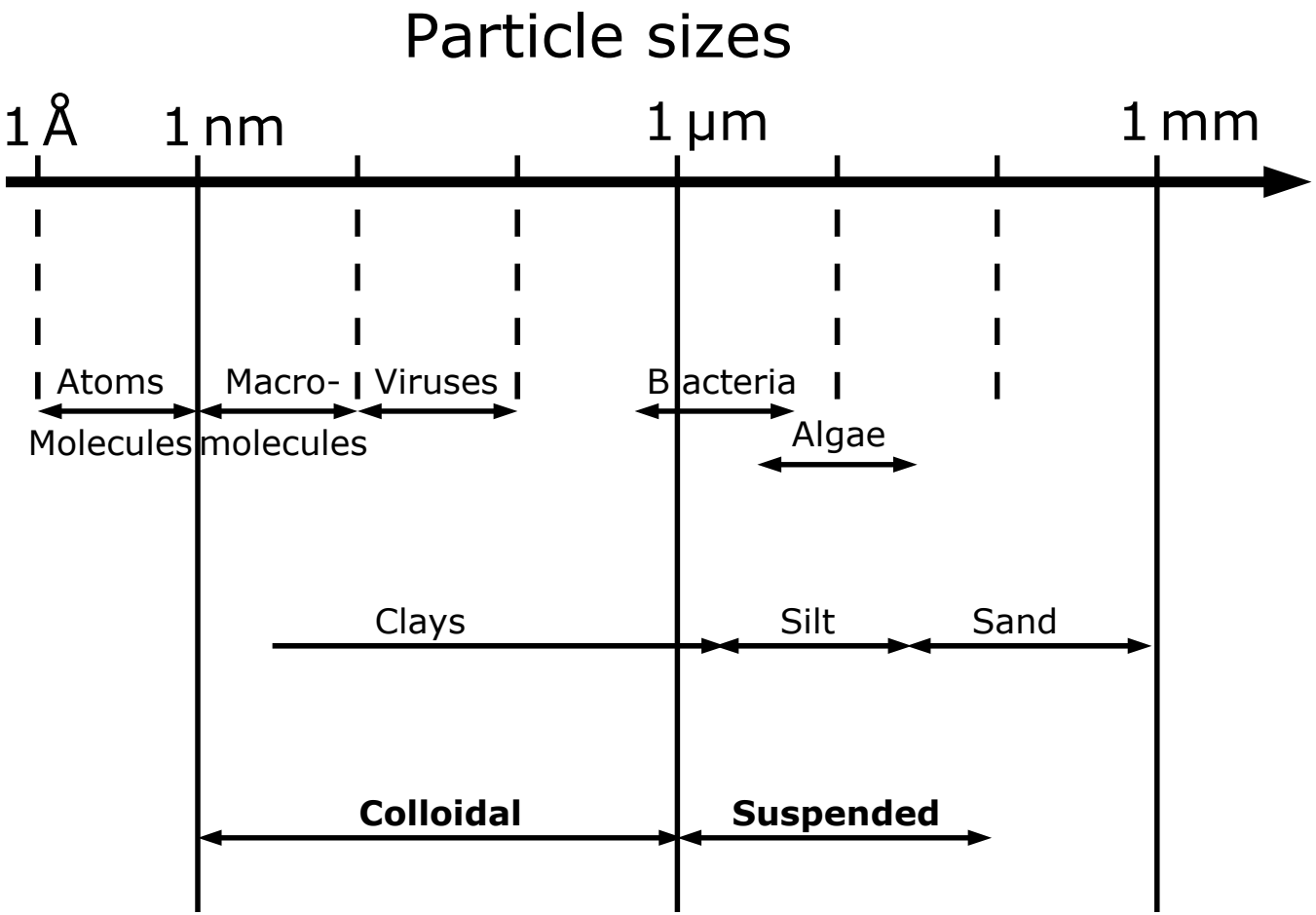

Equations for fluid motions

- Fluid motions described by the continuity and Navier-Stokes equations, given by (for incompressible flows):

$$\nabla \cdot \mathbf{v} = 0$$

$$\left(\frac{\partial \mathbf{v}}{\partial t} + \mathbf{v} \cdot \nabla \mathbf{v} \right) = -\frac{1}{\rho} \nabla p + \nu \nabla^2 \mathbf{v} + \mathbf{F}$$

- Turbulent flows:

  $\Rightarrow$ Fluctuations of $\mathbf{v}(t,x)$ in time and in space over a continuous wide range of scales

- Computational Fluid Dynamics (CFD):
  solving Navier-Stokes equations using numerical methods

Modelling approaches for fluid motions

- Various numerical methods can be used for turbulent flow simulations:
  - Direct Numerical Simulation (DNS):

    Exact solutions over the entire range of turbulent scales
    High computational costs (proportional to Re^3)
    Untractable in complex 3D cases

  - Large-Eddy Simulation (LES):

    Solving only the largest scales of turbulence, model for the small-scales
    Lower computational costs than DNS but higher than RANS

  - Reynolds-Averaged Navier-Stokes (RANS):

    Solving only the first two moments of the velocity field: $\mathbf{v} = \langle \mathbf{v} \rangle + \mathbf{v}'$
    $\Rightarrow$ Time-averaged velocity $\langle \mathbf{v} \rangle$ given by the mean Navier-Stokes equation:

$$\left(\frac{\partial \langle \mathbf{v} \rangle}{\partial t} + \langle \mathbf{v} \rangle \cdot \nabla \langle \mathbf{v} \rangle \right) = -\nabla \cdot \left(\langle \mathbf{v}' \otimes \mathbf{v}' \rangle \right) - \frac{1}{\rho} \nabla \langle p \rangle + \nu \nabla^2 \langle \mathbf{v} \rangle + \langle \mathbf{F} \rangle$$

    Model for the Reynolds stress tensor $\langle \mathbf{v}' \otimes \mathbf{v}' \rangle$
    Tractable in complex 3D situations

Modelling approaches to surface fouling

- Adsorption model (no fluid)
  - RSA
  - Ballistic models
- Models with fluid transport
  - Eulerian approaches
  - Lattice-based Monte-Carlo methods
  - Lagrangian approaches
    - Molecular Dynamics
    - Distinct Element Methods
    - Langevin Dynamics
    - Brownian Dynamics
    - Dissipative Particle Dynamics
    - One-particle pdf approach
- Classification of the modelling approaches

Random Sequential Adsorption (RSA)

- Principle
  - Sequential deposition (one particle at a time)
  - Particle position generated randomly above a plate
  - Irreversible deposition if no contact with already adsorbed particles
  - Refinements to account for lateral particle-particle interactions
  - Refinements for the particle-surface interactions
  - Refinements for particle diffusion (DRSA)

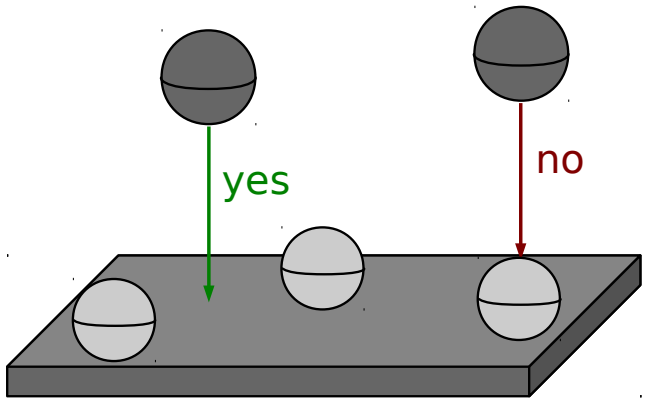

- Main results
  - Study of the kinetics of monolayer formation
  - Study of blocking effects
    $\rightarrow$ Extraction of constitutive laws

Return

Ballistic models

- Principle
  - Sequential deposition (one particle at a time)
  - Particle position generated randomly above a plate
  - Rolling motions of particles upon deposition

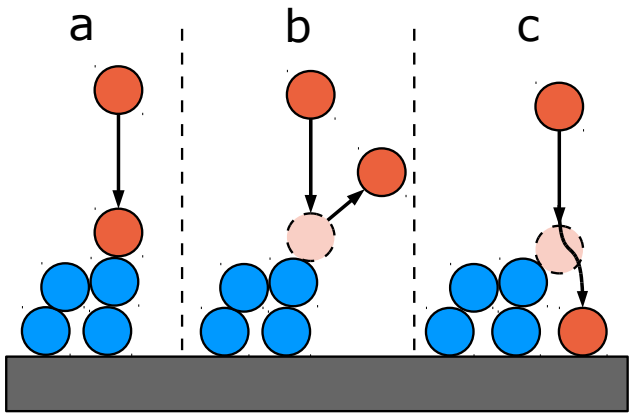

- Main results
  - Study of the deposit morphology
    $\rightarrow$ Random close packings with rolling motions
    $\rightarrow$ Random loose packings without rolling motions

Return

Eulerian approaches

- Principle
  - Use of convective-diffusion equation for particle transport

$$\frac{\partial c}{\partial t} + \nabla \cdot (c\mathbf{v}) = \nabla \cdot (D \cdot \nabla c - c\tau \mathbf{F})$$

with c the particle concentration, $\mathbf{v}$ the fluid velocity, D the diffusion matrix (including the hydrodynamic and possible turbulent effects), τ the characteristic timescale and $\mathbf{F}$ the external forces (such as DLVO interactions)

$\rightarrow$ Closure relations for D and $\mathbf{F}$ (range of validity?)

  - Boundary conditions

Perfect sink model ($c = 0$ at the surface), non-penetration models (flux $j = 0$ at the surface), etc.

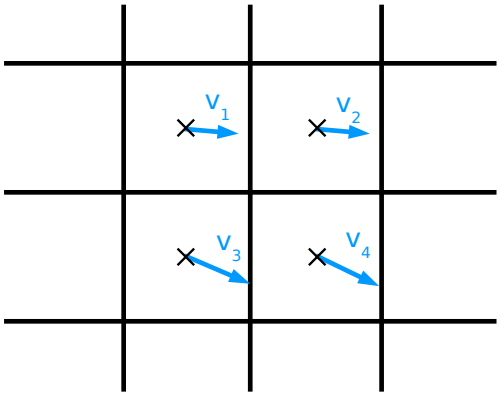

Eulerian approaches

- Principle
  - Use of convective-diffusion equation for particle transport

$$\frac{\partial c}{\partial t} + \nabla \cdot (c\mathbf{v}) = \nabla \cdot (D \cdot \nabla c - c\tau \mathbf{F})$$

    with c the particle concentration, $\mathbf{v}$ the fluid velocity, D the diffusion matrix (including the hydrodynamic and possible turbulent effects), τ the characteristic timescale and $\mathbf{F}$ the external forces (such as DLVO interactions)

    $\rightarrow$ Closure relations for D and $\mathbf{F}$ (range of validity?)

  - Boundary conditions

    Perfect sink model ($c = 0$ at the surface), non-penetration models (flux $j = 0$ at the surface), etc.

- Main results
  - Fast evaluation of macroscopic clogging properties
    $\rightarrow$ Good evaluations of breakthrough curves and jamming limits
  - Only limited information on macroscopic details (here concentration)
  - No insights into microscopic details

Return

Lattice-Based Monte-Carlo methods

- Principle
  - Simple "Toy" models for particle transport
  - Discretisation over a lattice
    $\rightarrow$ Particle motions according to probabilities to move from one site to another site
  - Macroscopic properties obtained through averaging over many realisations

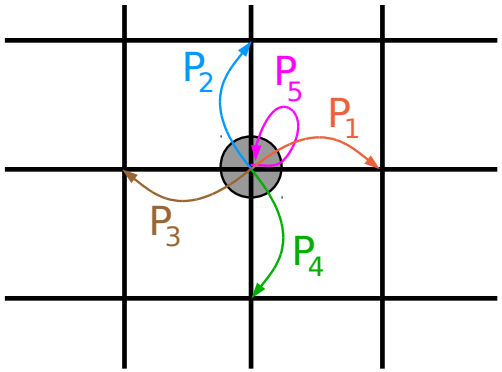

- Main results
  - Access to mesoscopic details of multilayer formation (local mechanisms)
  - Good predictions of the monolayer formation
  - Dependence of multilayer growth on electrostatic properties recovered

Return

Molecular Dynamics (MD)

- Principle
  - Solving directly the Newtonian equations of motion for all molecules:

$$m_i \frac{dv_i}{dt} = \sum_j F_{j \to i}$$

with $F_{j \to i}$ the force of particle labelled j on the one labelled i

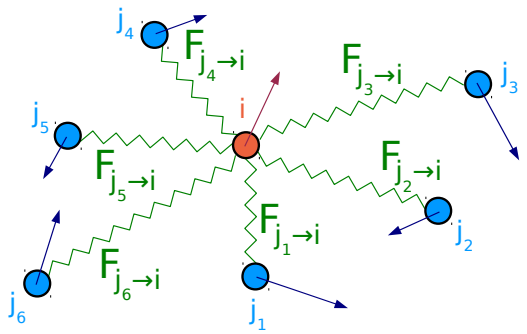

- Main results
  - Detailed microscopic results
  - But only tractable for small system (due to high computational costs)
    →Small time steps (for rapid fluctuations)
    → Very dilute suspensions (limited number of particles)

Return

Distinct Element Methods (DEM)

- Principle
  - Solving directly the equations of both translational and rotational motions for all particles:

$$m_i \frac{dv_i}{dt} = \sum_j F_{j \to i}$$

$$I_i \frac{d\Omega_i}{dt} = \sum_j M_{j \to i}$$

with m_i the particle mass, v_i the particle velocity, $F_{j \to i}$ the forces acting on the particle, I_i the particle inertia, Ω_i the particle angular velocity and $M_{j \to i}$ the torque exerted on the particle.

- Main results
  - DEM simulation of particulate clogging in porous media
  - Study on the deposit morphology
  - But, as for MD simulations, only tractable for small system (due to high computational costs)

Return

Langevin Dynamics

- Principle
  - Langevin-type equations of particle motion

$$m_i \frac{dv_i}{dt} = \sum_j \widetilde{F}_{j \to i} + \eta_i(t) - \gamma_i v_i$$

with $\widetilde{F}_{j \to i}$ the forces with slow variations acting on particles, η_i a noise term for rapidly fluctuating variables and $\gamma_i vi$ the fluid drag force.

Return

Brownian Dynamics

- Principle
  - Limiting case of LD with a force-balance approach:

$$0 = \sum_j \widetilde{F}_{j\to i} + \eta_i(t) - \gamma_i v_i$$

with $\widetilde{F}_{j\to i}$ the forces with slow variations acting on particles, η_i a noise term for rapidly fluctuating variables and $\gamma_i vi$ the fluid drag force.
leading to a formulation on particle positions $X_{p,i}$ only:

$$dX_{p,i} = \frac{1}{\gamma_i} \sum_j \widetilde{F}_{j\to i} + \sqrt{2D} dW_i$$

  - Simplifications:
    Sequential BD methods (consecutive single particle deposition)
    Ranged BD methods (interparticle interactions only within a limited distance)

- Main results
  - Microscopic details (such as the shadow effect)
  - Multilayer and monolayer formation captured by the coupling between particle-particle, particle-fluid and particle-surface interactions.

Return

Dissipative Particle Dynamics

- Principle
  - Description of the motion of a collection of DPD mesoscale "particles", representing an ensemble of colloidal particles

$$m_i \frac{d\widehat{v}_i}{dt} = \sum_j \left(\widehat{F}^C_{j\to i} + \widehat{F}^D_{j\to i} + \widehat{F}^R_{j\to i} \right) + \widehat{F}_{ext}$$

with $\widehat{v}_i$ the mesoscale "particle" velocity, $\widehat{F}^C_{j\to i}$, $\widehat{F}^D_{j\to i}$and $\widehat{F}^R_{j\to i}$ the conservative, dissipative and random (Brownian) forces (if particle j is within the radius of influence of particle i), and with $\widehat{F}_{ext}$ the external forces

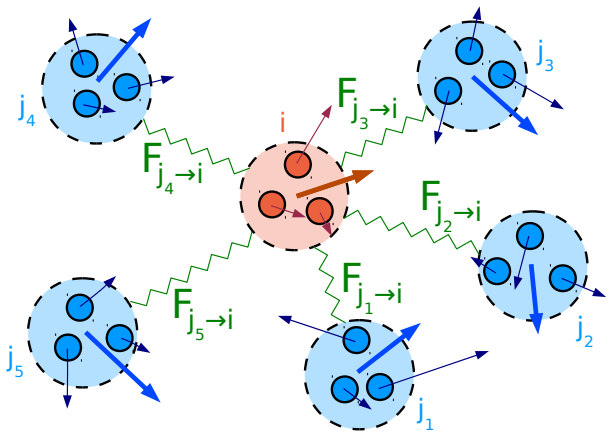

Dissipative Particle Dynamics

- Principle
  - Description of the motion of a collection of DPD mesoscale "particles", representing an ensemble of colloidal particles

$$m_i \frac{d\widehat{v}_i}{dt} = \sum_j \left(\widehat{F}^C_{j\to i} + \widehat{F}^D_{j\to i} + \widehat{F}^R_{j\to i} \right) + \widehat{F}_{ext}$$

with $\widehat{v}_i$ the mesoscale "particle" velocity, $\widehat{F}^C_{j\to i}$, $\widehat{F}^D_{j\to i}$and $\widehat{F}^R_{j\to i}$ the conservative, dissipative and random (Brownian) forces (if particle j is within the radius of influence of particle i), and with $\widehat{F}_{ext}$ the external forces

- Main results
  - Coarse-grained molecular dynamics method
  - Correct predictions of the accumulation of platelet in blood flows

Return

One-particle pdf approach

- Principle
  - Equation of motions described using modelled forces, obtained through mean-field approaches
    $\rightarrow$ State vector associated to each particle

$$m_i dv_i = \overline{F_i}\ dt + K_i\ dW_i$$

with $\overline{F_i}$ and the diffusion coefficients K_i are models for the forces acting on particles.

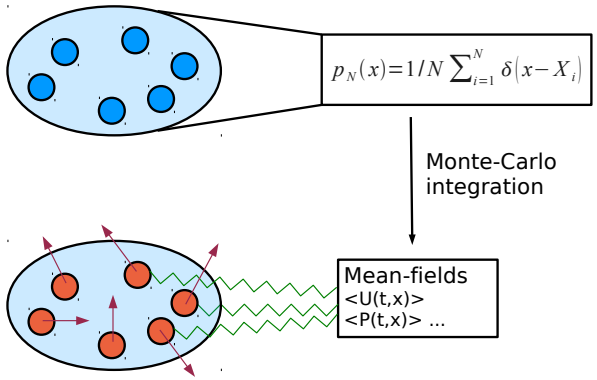

- Main advantages
  - Tractable in 3-D industrial cases

Return

Classification of the modelling approaches to surface fouling

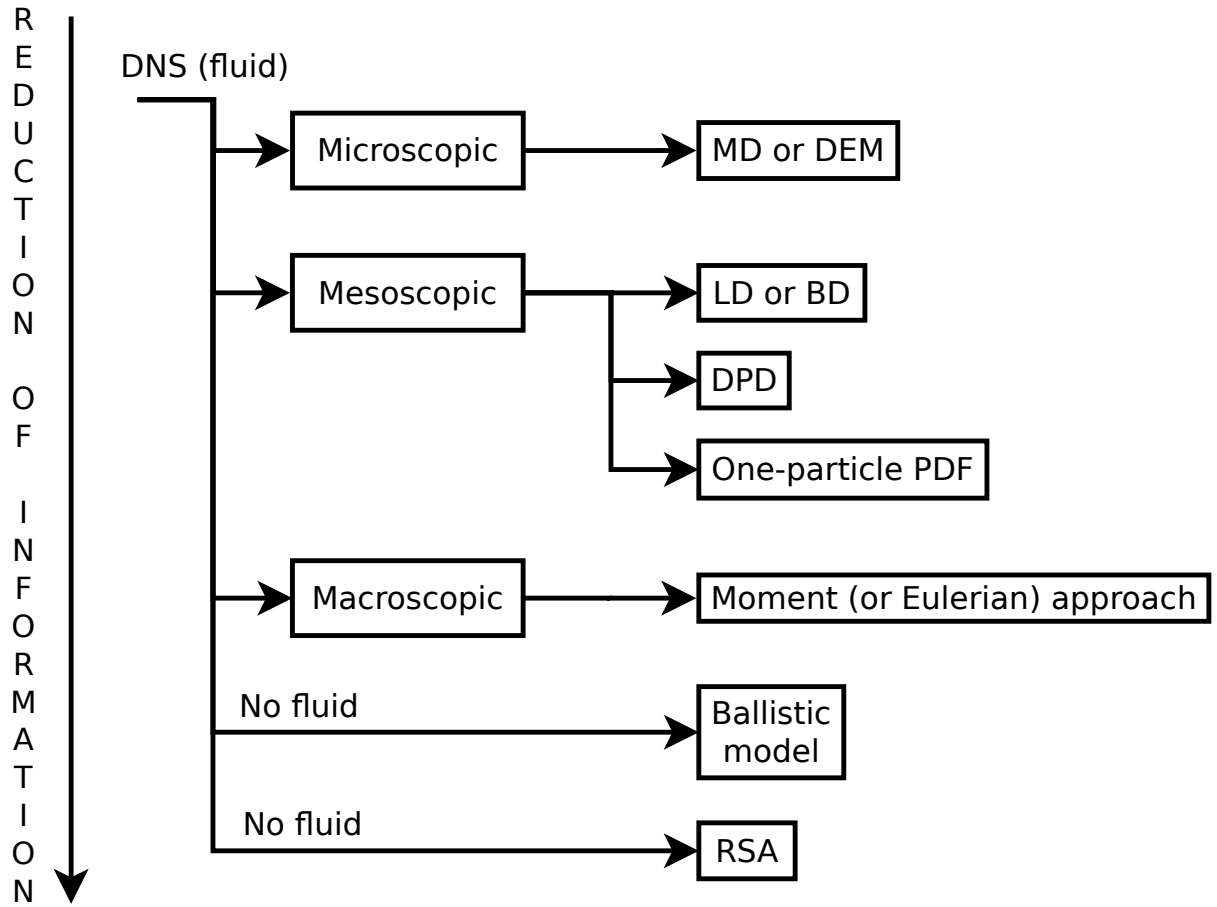

Classification of the modelling approaches to surface fouling (2)

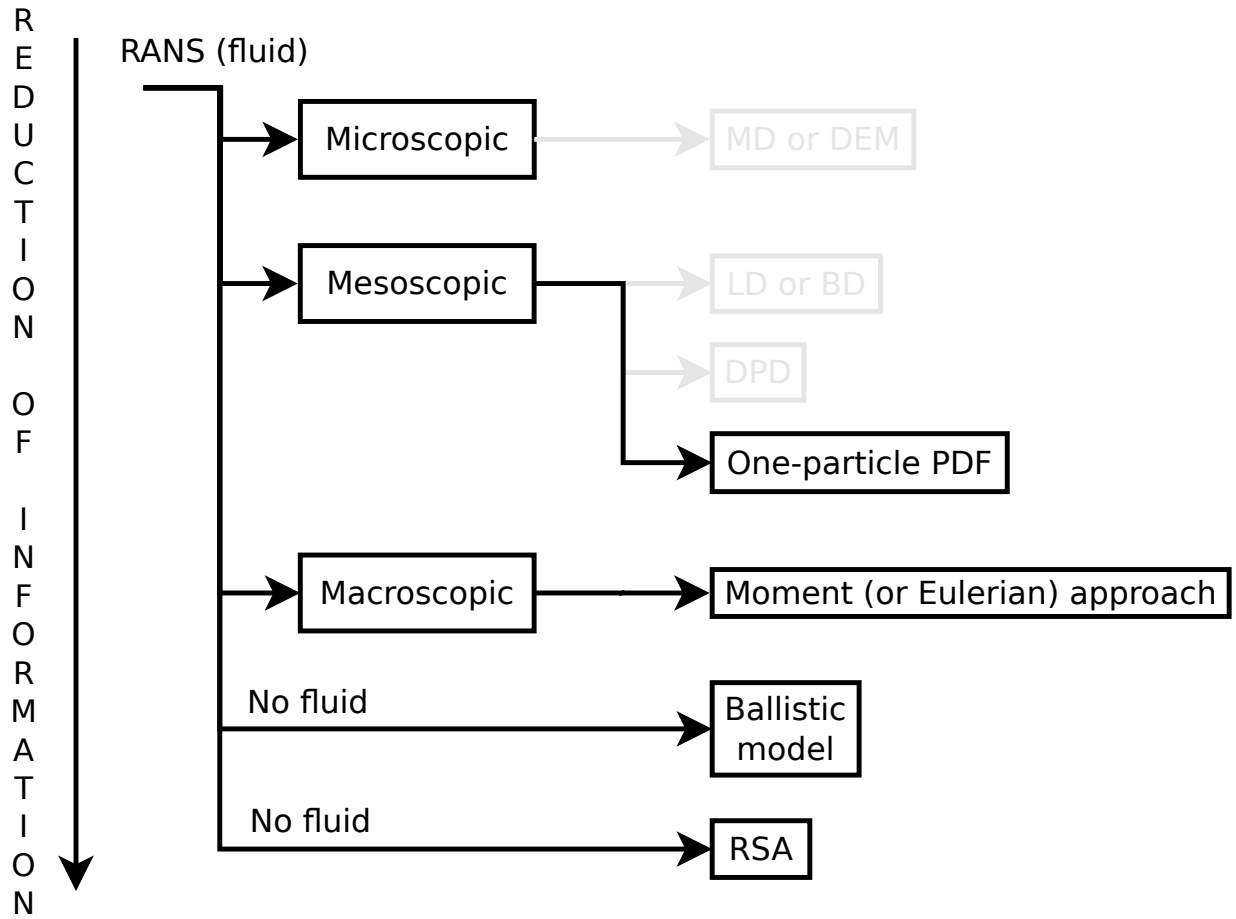

$\Rightarrow$ Need for consistent approaches for fluid and particle motions

Return

Equations of particle motions

Newton's law, which for negligible relative Reynolds number ($R_p = d_p U_R / \nu_f$, where $U_R = U_s - U_p$) reduces to:

$$dx_p = U_p dt$$
$$dU_p/dt = F_1 + F_2$$

- Undisturbed field: F_1
  - Pressure gradient forces $\frac{\pi d_p^3}{6} \rho_f \frac{DU_s}{Dt}$
  - Buoyancy forces $\frac{\pi d_p^3}{6} (\rho_p - \rho_f) g$
- Disturbance field: F_2
  - Drag forces $3\pi d_p \rho_f \nu_f (U_s - U_p)$
  - Added-mass forces (inertia added to the fluid due to particle acceleration) $\frac{\pi d_p^3}{12} \rho_f (\frac{DU_s}{Dt} - \frac{dU_p}{dt})$
  - Basset forces (viscous effects + boundary layer development due to particle acceleration) : $\frac{3d_p^2}{2} \rho_f \sqrt{\pi \nu_f} (\int_{-\infty}^{t} \frac{d}{d\tau} (U_s - U_p) \frac{d\tau}{\sqrt{t-\tau}})$

Equations of particle motions (2)

- For heavy particle $\rho_p \gg \rho_f$:
  Drag and gravity forces are predominant

$$dx_p = U_p dt$$
$$dU_p = \frac{U_s - U_p}{\tau_p} dt + g \ dt$$

  where τ_p is the particle relaxation time scale related to drag forces:
  $\tau_p = \frac{4\rho_p d_p}{3\rho_f C_D |U_R|} \xrightarrow{\rho_p \gg \rho_f} \frac{\rho_p d_p^2}{18\rho_f}$

- For colloidal particles:
  Gravity is negligible compared to Brownian motion

$$dx_p = U_p dt$$
$$dU_p = \frac{U_s - U_p}{\tau_p} dt + K_{Br} \ dW$$
$$\text{with } K_{Br} = \sqrt{\frac{2k_B T}{m_p \tau_p}}$$

Formalism for the one-particle pdf approach

Lagrangian formalism

$$dx_{p,i} = U_{p,i}dt$$
$$dU_{p,i} = \frac{U_{s,i}-U_{p,i}}{\tau_p}dt + K_{Bro}dW_i'$$
$$dU_{s,i} = A_i(t,U_{s,i})dt + B_i(t,U_{s,i})dW_i$$

- Drift term: forces with slow variations
  $A_i(t,U_{s,i}) = -\frac{1}{\rho_f}\frac{\partial\langle P\rangle}{\partial x_i} + (\langle U_{p,j}\rangle - \langle U_{p,j}\rangle)\frac{\partial\langle U_{f,i}\rangle}{\partial x_j} - \frac{U_{s,i}-\langle U_{f,i}\rangle}{T^*_{L,i}}$
  where T^*_L is the fluid Lagrangian time scale (* refers to modifications due to crossing-trajectory effects).
- Diffusion term: forces with rapid fluctuations
  $B_i(t,U_{s,i}) = \sqrt{\langle\varepsilon\rangle(C_0 b_i \tilde{k}/k + 2/3(b_i\tilde{k}/k - 1))}$
  where $b_i = \frac{T_L}{T^*_{L,i}}$ is the correction factor from Csanady's formulae
  and $\tilde{k} = \frac{3}{2}\frac{\sum_{i=1}^3 b_i\langle u^2_{f,i}\rangle}{\sum_{i=1}^3 b_i}$ is a modified kinetic energy accounting for anisotropy in the turbulent kinetic energy.

Near-wall hydrodynamic model

- 1D Formulation accounting for the random succession of near-wall coherent structures along particle trajectories
- Langevin equation for the wall-normal velocity V_p

$$dy_{p,i} = V_{p,i}\,dt$$
$$dV_{p,i} = \frac{V_{s,i} - V_{p,i}}{\tau_p}\,dt + K_{Bro}\,dW_i'$$

where the fluid velocity seen by the particle is described by a succession of motions:

$$V_s = -V_{struc} \qquad \textit{sweep}$$
$$V_s = V_{struc} \qquad \textit{ejection}$$
$$dV_s = -\frac{V_s}{T_L}\,dt + K_{ext}\,dW \qquad \textit{diffusion}$$
$$dV_s = A_{int}\left(y_p^+\right)dt - \frac{V_s}{T_L}\,dt + K_{int}\left(y_p^+\right)dW \qquad \textit{internal layer}$$

Van der Waals interactions: origin

- Interaction between spontaneous polarisations of nearby dipoles
  - Keesom interactions between two permanent dipoles

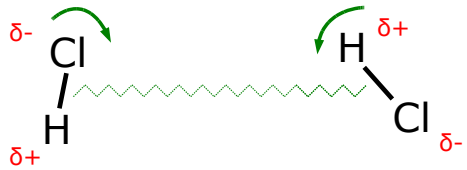

  - Debye interactions between one permanent dipole and a corresponding induced dipole
  - **London dispersion interactions between two transient dipoles**.

- Retardation:
  Arise when the separation distance is high, leading to a non-instantaneous interaction between dipoles (due to the finite light velocity)

Van der Waals interactions: modelling approaches

- Molecular scale:
  London molecule-molecule interaction $\propto 1/h^6$
- Macroscopic scale

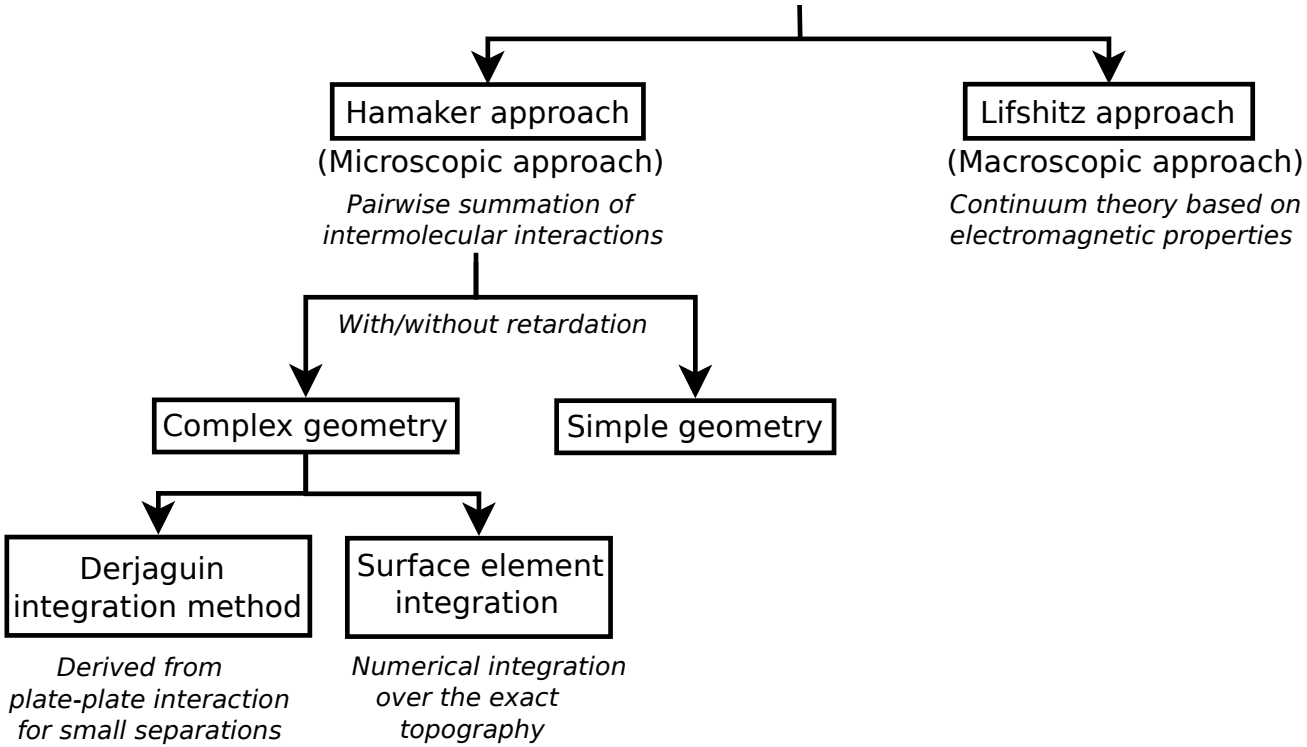

Electrostatic Double-Layer interactions: origin

- Origin of the electrical double-layer:
  Screening of the surface charge by ions present in the solution

  Description by the Stern-Grahame model:

Competition between:

- Chemical reactions occurring at the surface (ad/de-sorption of protons, or ions)
- Electrostatic affinity of ions in the solution (described by the Poisson-Boltzmann equation)

$$\nabla^2 \psi = -\frac{1}{\varepsilon_r \varepsilon_0} \sum_i n_i^0 z_i e \, exp\left(\frac{-z_i e \psi}{k_B T}\right)$$

(ε_0: permittivity of vacuum, ε_r: material dielectric permittivity, n_i^0: number density of ions of valency z_i, e: elementary charge, k_B: Boltzmann constant, T: temperature).

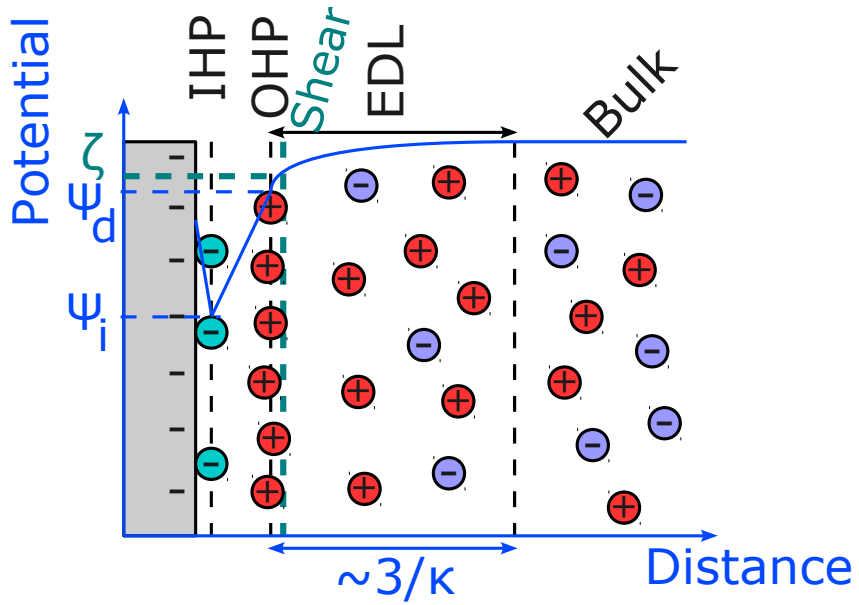

Electrostatic Double-Layer interactions: modelling approaches

- Macroscopic interactions:

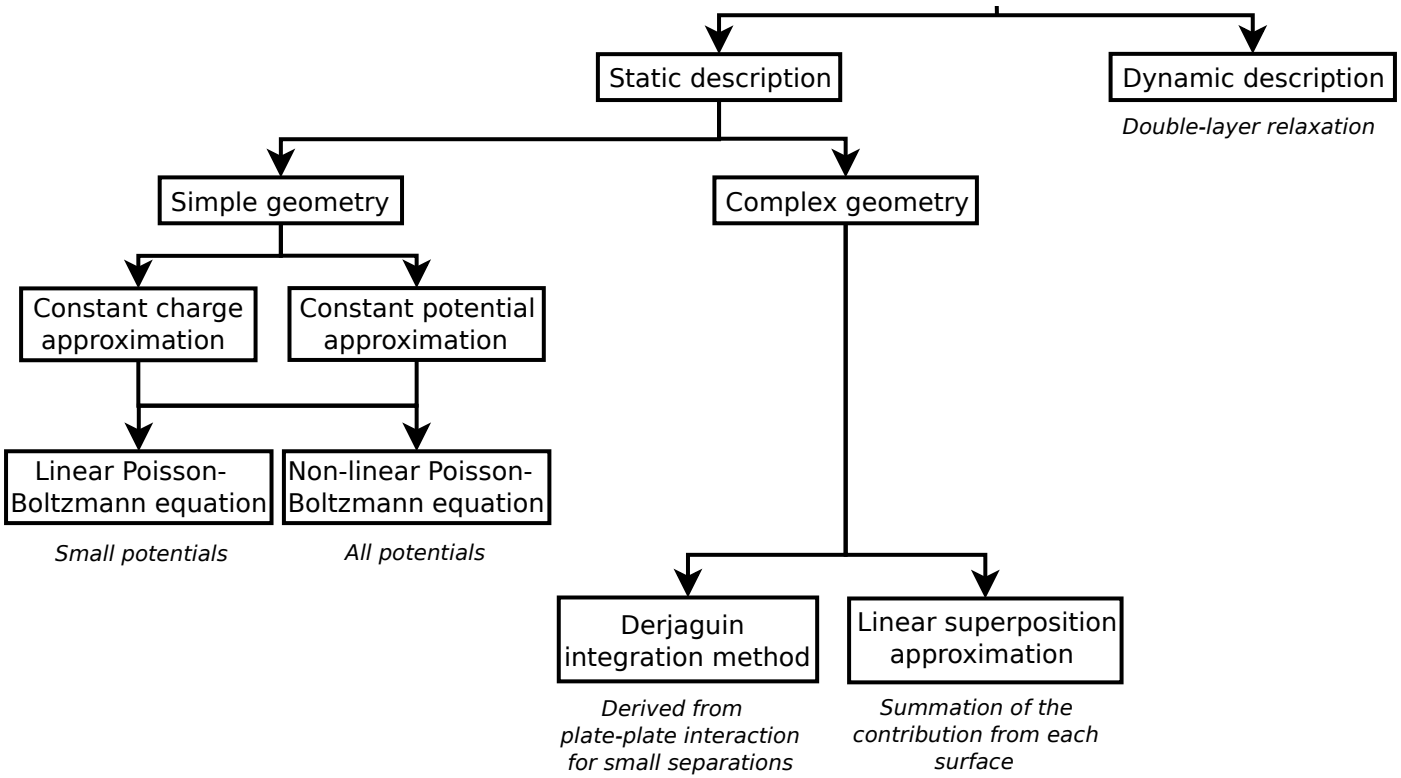

DLVO interaction: VDW formulae

- Sphere-plate geometry: Gregory formula valid at small separations, and Czarnecki formula valid at larger separations

$$U_{SP}^{VdW} = \frac{-A_{Ham} R_{part}}{6h} \times \left(\frac{1}{1 + \frac{14h}{\lambda} + \frac{5\pi h^3}{4.9\lambda R_{part}^2}} \right) \text{ if } h < \frac{\lambda}{2\pi}$$

$$\begin{aligned} U_{SP}^{VdW} = & A_{Ham} \frac{2.45\lambda}{60\pi} \left(\frac{h - R_{part}}{h^2} - \frac{h + 3R_{part}}{(h + 2R_{part})^2} \right) \\ & - A_{Ham} \frac{2.17\lambda^2}{720\pi^2} \left(\frac{h - 2R_{part}}{h^3} - \frac{h + 4R_{part}}{(h + 2R_{part})^3} \right) \\ & + A_{Ham} \frac{0.59\lambda^3}{5040\pi^3} \left(\frac{h - 3R_{part}}{h^4} - \frac{h + 5R_{part}}{(h + 2R_{part})^4} \right) \end{aligned}$$

- Sphere-sphere geometry: Gregory formula valid at small separations

$$U_{SA}^{VdW} = \frac{-A_{Ham} R_{part} R_{asp}}{6h(R_{part} + R_{asp})} \times \left(1 - \frac{5.32h}{\lambda} \ln \left(1 + \frac{\lambda}{5.32h} \right) \right)$$

DLVO interaction: EDL formulae

- Sphere-sphere and sphere-plate geometries: Bell et al formula valid at all separations, for small potentials and $\kappa R_i \geq 5$

$$U_{SA}^{EDL} = 2\pi\varepsilon_0\varepsilon_R \left(\frac{k_B T}{ze}\right)^2 \times \frac{R_{part} R_{asp}(r - R_{part})(r - R_{asp})}{r[(R_{part} + R_{asp})r - R_{part}^2 - R_{asp}^2]} \times [\Omega_1 \ln(1 + \Gamma) + \Omega_2 \ln(1 - \Gamma)]$$

with the reduced potentials $\Phi = ze\varphi / k_B T$ and:

$$\Omega_1 = \Phi_1^2 + \Phi_2^2 + \Lambda\Phi_1\Phi_2$$

$$\Omega_2 = \Phi_1^2 + \Phi_2^2 - \Lambda\Phi_1\Phi_2$$

$$\Lambda = \sqrt{\frac{R_{part}(r - R_{part})}{R_{asp}(r - R_{asp})}} + \sqrt{\frac{R_{asp}(r - R_{asp})}{R_{part}(r - R_{part})}}$$

$$\Gamma = \sqrt{\frac{R_{part} R_{asp}}{(r - R_{part})(r - R_{asp})}} \times e^{\kappa(R_{part} + R_{asp} - r)}$$

Lift of the small potential approximations with the potential from Ohshima et al:

$$Y = 8 \times tanh\left(\frac{\Phi}{4}\right) \times \left(1 + \sqrt{1 - \frac{2R_i\kappa + 1}{(R_i\kappa + 1)^2} tanh^2\left(\frac{\Phi}{4}\right)}\right)^{-1}$$

Dynamics of the DLVO interaction: charge regulation

EDL interactions: overlap of two double-layers

- Static interaction:
  - Constant potential CP approximation (used here)
  - Constant charge CC approximation
- Dynamic interaction:
  Variations of charge and potential upon interaction
  - Constant regulation CR approach:
    Use of a regulation parameter as a linearised sum of the CP and CC interactions
  - Electrostatic and chemical approach:
    Kinetics of the chemical reactions at the surface
    Equations for the electrostatic affinity of ions in the double-layer
- Limits (restraining its use in the present case):
  - Increase of the energy barrier
  - Intricate coupling with surface roughness

Existing models for adhesion forces

Various methods exist to describe the adhesion between two bodies:

- Surface energy (γ) methods
  - JKR model:
    Adhesion force inside the contact area (given by surface deformation)
    Valid provided that $\mu_T = \left(R_{part}\Delta\gamma^2/(E^2 z_0^3)\right)^{1/3} \gg 1$ (soft spheres)

$$F_{ad} = 3\pi \frac{R_1 R_2}{R_1 + R_2}\gamma$$

  - DMT model:
    Inclusion of non-contact forces in the vicinity of the contact area
    Valid provided that $\mu_T \leq 1$ (hard spheres)

$$F_{ad} = 4\pi \frac{R_1 R_2}{R_1 + R_2}\gamma$$

  - Maugis-Pollock model:
    Transition from JKR to DMT theories
- Hamaker approach
  VDW interaction energy at contact $z_0 = 0.169\ nm$ (no deformation)

Model for surface roughness

The attachment step has been refined to account for surface roughness (see *Henry et al, Langmuir, 2011, Vol. 27(8), pp. 4603-4612*)

- Generation of surface roughness:

  Rough surfaces described by smooth plates covered by spherical asperities

  - Hemispherical asperities only within a certain cut-off radius (interactions are negligible further than $10/\kappa$):

    $$S_{eff} = 2.5\pi(2R_{part} + R_{asp} + 10/\kappa)(R_{asp} + 10/\kappa)$$

  - Number of asperities within the surface S_{eff} given by a Poisson distribution with mean $\frac{S_{eff} \times S_{cov}}{\pi R_{asp}^2}$
  - Hemispherical asperities placed randomly on the surface
  - Polydispersion in the size of asperities

  Other approach

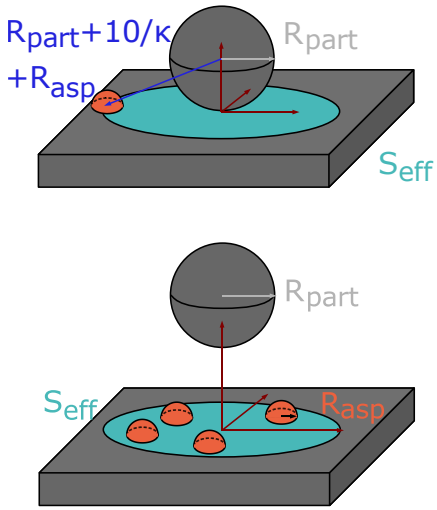

⇒ **Statistical representation using two physical parameters:** R_{asp} **and** S_{cov}

Model for the interaction energies between rough surface

The attachment step has been refined to account for surface roughness (see *Henry et al, Langmuir, 2011, Vol. 27(8), pp. 4603-4612*)

- Model for surface roughness:
  - Hemispherical asperities only within a certain cut-off radius (interactions are negligible further away)
  - Hemispherical asperities placed randomly on the surface

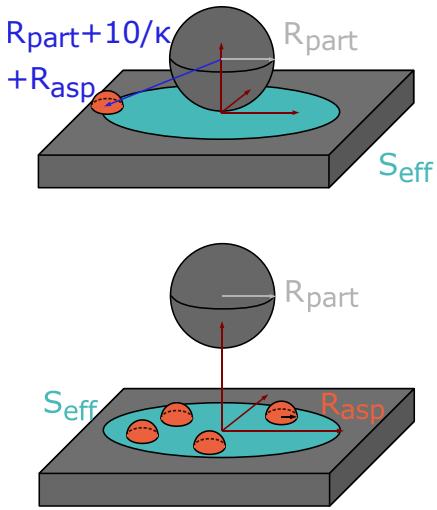

- Interaction energy:
  - Still described using the DLVO theory
  - Assuming the additivity of interaction energies: formula

$$U^{DLVO}_{Sphere-Surface} = (1 - S_{cov}) U^{DLVO}_{Sphere-plate} + \sum_{asperities} U^{DLVO}_{Sphere-asperity}$$

⇒ **Statistical information (such as the probability density function PDF, mean, max, min) on the energy barrier using Monte-Carlo evaluations**